

Detecting Relativistic Doppler in Galaxy Clustering with Tailored Galaxy Samples

Federico Montano^{1,2,*} and Stefano Camera^{1,2,3,4,†}

¹*Dipartimento di Fisica, Università degli Studi di Torino, Via P. Giuria 1, 10125 Torino, Italy*

²*INFN – Istituto Nazionale di Fisica Nucleare, Sezione di Torino, Via P. Giuria 1, 10125 Torino, Italy*

³*INAF – Istituto Nazionale di Astrofisica, Osservatorio Astrofisico di Torino, Strada Osservatorio 20, 10025 Pino Torinese, Italy*

⁴*Department of Physics & Astronomy, University of the Western Cape, Cape Town 7535, South Africa*

We present a method to obtain a high-significance detection of relativistic effects on cosmological scales. Measurements of such effects would be instrumental for our understanding of the Universe, as they would provide a further confirmation of the validity of general relativity as the correct description of the gravitational interaction, in a regime very far from that of strong gravity, where it has been tested to exquisite accuracy. Despite its relevance, detection of relativistic effects have hitherto eluded us, mainly because they are stronger on the largest cosmic scales, plagued by cosmic variance. Our work focusses on the cosmological probe of galaxy clustering, describing the excess probability of finding pairs of galaxies at a given separation due to them being part of the same underlying cosmic large-scale structure. In particular, we focus on the two-point correlation function of the distribution of galaxies in Fourier space—the power spectrum—where relativistic effects appear as an imaginary contribution to the real power spectrum. By carefully tailoring cuts in magnitude/luminosity, we are able to obtain two samples (bright and faint) of the same galaxy population, whose cross-correlation power spectrum allows for a detection of the relativistic contribution well above a significance of 5σ .

Introduction. Gravity is the force that mostly drives the evolution of the Universe, since it is the fundamental interaction that can act on cosmic distances. Therefore, our understanding of its properties is paramount for cosmology. As such, the current concordance cosmological model is rooted in the theory of general relativity (GR). Despite GR being supported by several stunning experimental observations [1–7], it is still poorly tested in the extremely-weak field regime of cosmological scales. In this context, a measurement of an effect due to GR coming from cosmology would represent another amazing success of Einsteinian gravity, whereas departures from GR would be a window into the intriguing ‘modified gravity’ scenario [8, 9].

The large-scale structure of the Universe offers an important test bench for gravity theories. The properties of galaxy clustering tell us about the driving force of cosmological evolution, simply because a clumpy Universe like the one we live in has to be the result of ages of gravitational accretion, starting from nearly-homogeneous primordial stages. In particular, a statistical investigation of the distribution of a certain tracer, e.g. a type of galaxy, can display signatures of various effects that affect the observed position and magnitude of sources in the sky. We ascribe most of these phenomena to the fact that galaxy surveys actually map cosmic structures in observed redshift space, rather than in real space. Also, gravitational lensing is known to affect the observed clustering of sources, because photons from distant galaxies are scattered by the intervening large-scale structure on their journey towards us. Other corrections that should be taken into account are so-called relativistic effects, amongst which the dominant one is a relativistic Doppler term. The amplitude of such Doppler term is itself affected by gravitational lensing effects and the evolution of the target galaxy population.

In this paper, we present a strategy to detect the relativistic Doppler through the study of galaxy clustering. Following the idea first proposed by Bonvin *et al.* [10, see also 11, 12], we divide a galaxy population according to observed flux density (namely, according to luminosity) in order to work with two complementary selections of the same sample. The faint and bright samples thus obtained are by construction independent and are hence two promising candidates for a cross-correlation study—i.e. the analysis of the covariance between the galaxy distributions in the two sub-samples.

Since relativistic effects are subdominant on small scales, which are also most affected by the non-linear growth of structures, it is convenient to isolate small scales from large scales. The best way to do so is by studying clustering in Fourier space, through the Fourier-space galaxy two-point correlation function, viz. the power spectrum. Hitherto, a detection of the Doppler term via power spectrum measurement has not been achieved yet, primarily because the very large scales, where relativistic effects are stronger, are afflicted by a dramatically low statistical sampling, which plagues experimental observations. To overcome this issue, McDonald [13] proposed to use cross-correlations, due to them featuring a less steep scale-dependence of the Doppler contribution. A further complication, albeit an engaging opportunity, stems from the fact that the relativistic effects are sample-dependent, therefore different galaxy populations display different contributions in their power spectra. For this reason, a search for tailored galaxy samples, like the one we carry out in our work, appears to be useful in the efforts to provide a detection of relativistic Doppler with the upcoming observational campaigns.

Definitions. The leading local contributions to the number density contrast of galaxy counts read [13–18]

$$\Delta(\mathbf{x}) = b\delta(\mathbf{x}) - \frac{1}{\mathcal{H}}\partial_{\parallel}v_{\parallel}(\mathbf{x}) - \alpha v_{\parallel}(\mathbf{x}), \quad (1)$$

with b the linear bias, δ the matter density contrast (in comoving-synchronous gauge), \mathcal{H} the conformal Hubble factor, \mathbf{v} the peculiar velocity field, and subscript ‘ \parallel ’ denoting the

* federico.montano@edu.unito.it

† stefano.camera@unito.it

component of a vector along the line of sight.¹ Above,

$$\alpha := \frac{\mathcal{H}'}{\mathcal{H}^2} - \mathcal{E} + 2Q - 2\frac{Q-1}{\mathcal{H}} + 1 \quad (2)$$

is the overall amplitude of the Doppler term, with a prime denoting derivation with respect to conformal time, and \mathcal{E} and Q , respectively, the so-called evolution and magnification bias [15].² They are defined by

$$Q = -\frac{\partial \ln n(z; L > L_c)}{\partial \ln L_c}, \quad \mathcal{E} = -\frac{\partial \ln n(z; L > L_c)}{\partial \ln(1+z)}, \quad (3)$$

where $n(z; L > L_c)$ is the comoving number density of sources with a luminosity larger than L_c .

In Fourier space, Eq. (1) corresponds to

$$\Delta(\mathbf{k}) = \left(b + f\mu^2 + i\frac{\mathcal{H}}{k}\alpha f\mu \right) \delta(\mathbf{k}), \quad (4)$$

where $f := -d \ln \delta / d \ln(1+z)$ is the growth rate, μ is the cosine between the wavevector \mathbf{k} and the line of sight. In Eq. (4), $f\mu^2 \delta(\mathbf{k})$ is the well-known (linear) RSD term, whereas $i\mathcal{H}\alpha f\mu \delta(\mathbf{k})/k$ represents the relativistic Doppler contribution. Then, the power spectrum, i.e. the two-point correlation function in Fourier space, in the case of the auto-correlation of a tracer X (e.g. a certain galaxy population) is given by

$$P_{XX}(\mathbf{k}) = \left[(b_X + f\mu^2)^2 + \left(\frac{\mathcal{H}}{k}\alpha_X f\mu \right)^2 \right] P(k), \quad (5)$$

with $P(k)$ the (linear) matter power spectrum. The relativistic contribution is sub-dominant compared to the standard contributions (usually referred to as ‘Newtonian’), and due to its scaling $\propto k^{-2}$, relevant only on ultra-large scales.

Conversely, the situation is remarkably different for the cross-correlation between two different tracers. In general, we can write

$$P_{XY}(\mathbf{k}) = \left\{ (b_X + f\mu^2)(b_Y + f\mu^2) + \frac{\mathcal{H}^2}{k^2}\alpha_X\alpha_Y f^2\mu^2 + i\frac{\mathcal{H}}{k} \left[\alpha_X(b_Y + f\mu^2) - \alpha_Y(b_X + f\mu^2) \right] f\mu \right\} P(k), \quad (6)$$

¹ The minus sign in front of the two line-of-sight velocity terms comes from the line of sight being opposite to the direction of incoming photons.

² A varied notation in the literature calls for some clarification. What we denote here by α is exactly $-A_D$ in Maartens *et al.* [19], $1 - A$ in Maartens *et al.* [20] and $r\mathcal{H}\alpha_{GR}$ in Abramo and Bertacca [14]. All those definitions of the Doppler amplitude are dimensionless, contrarily to Paul *et al.* [21] who define it dimensionfully, in the form of Eq. (2) modified as $\alpha \rightarrow (\alpha - 1)\mathcal{H}$. The presence or absence of a 1 in the definitions just mentioned is related to either enforcing or not the validity of Euler’s equation. Regarding evolution bias, we prefer to use the letter \mathcal{E} versus other symbols used in the literature (e.g. b_e , b_{evo} , f_{evo}), to reduce clutter when adding further subscripts. Finally, for magnification bias, other common notations are $s = 2Q/5$ or, globally, $b_{mag} = 2 - 5s$ [e.g. 22, see also Maartens *et al.* 19 for a thorough review of evolution and magnification biases].

which refers to the cross-correlation power spectrum if $X \neq Y$ and resorts to Eq. (5) if $X = Y$. McDonald [13] first noted that, thanks to the not-vanishing imaginary term (which is inversely proportional to k), cross-correlation measurements are more promising than auto-correlations, as they allow the relativistic effects to be detected at somewhat intermediate scales. It is also interesting to note that, in the case of cross-correlations, the real part is symmetric through the exchange of the subscripts of the tracers, i.e. $X \leftrightarrow Y$, whilst the imaginary part is anti-symmetric. For this reason, we can always write $P_{XY}(\mathbf{k}) = P_{YX}(-\mathbf{k}) = P_{YX}^*(\mathbf{k})$, where an asterisk denotes complex conjugation.

Methodology. The relativistic Doppler effect depends mainly on the luminosity function of the observed galaxy sample, since the evolution and the magnification biases are both defined as a logarithmic derivative of the galaxy number density (see Eq. 3). To derive all those key quantities in a self-consistent way, we start from the galaxy luminosity function. In this work, we use models that present a factorised form for the luminosity function, $\phi(z, L) = \phi_*(z)g(L)$, where ϕ_* is a characteristic number density and L the luminosity. We adopt two models for the luminosity function: one of Schechter type and another coming from fits to observational data. In line with the nomenclature of Pozzetti *et al.* [23], we dub them *Model 1* and *Model 3*, respectively.

Operatively, we model the luminosity functions following the recipes outlined in Maartens *et al.* [19]. However, being the luminosity L an intrinsic property of galaxies, we cannot measure it directly. Experimental observations usually deal with flux density or apparent magnitude, and it is hence useful to move from a luminosity-based to a flux-based description. To this purpose, we take into account the observed density flux F as related to L by the well-known inverse-square law $F = L/(4\pi d_A^2)$, where $d_A(z)$ is the luminosity distance to redshift z . Henceforth, we use F , rather than L , to define galaxy samples.

To perform a cross-correlation analysis, instead of considering all the galaxies that are observed with a flux density higher than a fixed flux cut F_c , we consider two complementary galaxies selections. The former is composed of all the galaxies with an observed flux $F \in [F_c, F_s)$, where F_s is the value of the flux splitting between the two samples, and the latter contains all the galaxies with $F \geq F_s$. Thanks to this split, we are able to obtain two independent sub-samples (faint and bright) of the same galaxy population [see 10–12]. Labelling the faint, bright, and total samples respectively by subscripts ‘F’, ‘B’, and ‘T’, we have $n_T = n_F + n_B$, where n_X is the galaxy number density for tracer X .

Now, we have to calculate the different terms of Eqs. (5) and (6) for the two samples. As it is shown in Ferramacho *et al.* [24], it is possible to evaluate the linear galaxy bias, in the case of multiple samples, by means of a weighted average of the number densities of the individual biases. Hence, we can write $n_T b_T = n_B b_B + n_F b_F$. As we can see, the linear bias for the faint sample is a function of b_T and b_B , where in this work b_T and b_B are given by the cumulative bias for $H\alpha$ galaxies, which we model according to Pan *et al.* [25].

Concerning the magnification bias Q and the evolution bias \mathcal{E} , given by Eq. (3), we follow the procedure outlined in

Maartens *et al.* 19 to obtain the expressions for the faint, bright, and total samples. First, we notice that the definitions of \mathcal{Q}_B and \mathcal{E}_B are derived exactly as for the total sample by simply substituting F_c with F_s . On the other hand, for the faint sample, the expressions are somewhat different, due to the presence of the upper cut F_s . Specifically, we find the following original relations for the faint sample,

$$\mathcal{Q}_F = \frac{n_T}{n_T - n_B} \mathcal{Q}_T, \quad (7)$$

$$\mathcal{E}_F = -\frac{d \ln \phi_*(z)}{d \ln(1+z)} - \frac{d \ln L_*(z)}{d \ln(1+z)} \left(\mathcal{Q}_F - \frac{n_B}{n_T - n_B} \mathcal{Q}_B \right). \quad (8)$$

Detection significance. To quantify the presence of a relativistic Doppler signal in the data, and its significance, against the null hypothesis of no relativistic contributions, we rely on the $\Delta\chi^2$ test statistics. In our analysis, we use the theoretical prediction of Eq. (6) to produce synthetic data, and the $\Delta\chi^2$ therefore corresponds simply to the chi-square for a model with no Doppler term, against our synthetic data set that includes Doppler. As it will be apparent in the next section, it is useful to introduce three dummy, binary variables: A_N , A_K , and A_D . Respectively, they are responsible for switching off/on: the real-space clustering signal, proportional to the galaxy bias; linear RSD; and the Doppler term. Namely, we write

$$\Delta(\mathbf{k}) = \left(A_N b + A_K f \mu^2 + i A_D \frac{\mathcal{H}}{k} \alpha f \mu \right) \delta(\mathbf{k}). \quad (9)$$

Then, a given redshift bin centred in \bar{z}_i , the chi-square for the power spectrum reads

$$\chi_{XY}^2(\bar{z}_i) = \sum_{m,n} \frac{\left| P_{XY}^{(1,1,1)}(k_m, \mu_n; \bar{z}_i) - P_{XY}^{(1,1,0)}(k_m, \mu_n; \bar{z}_i) \right|^2}{\Delta P_{XY}^2(k_m, \mu_n; \bar{z}_i)}, \quad (10)$$

where we assumed, as customary, that the covariance matrix is diagonal in k -, μ -, and z -space, having denoted by ΔP_{XY}^2 the variance on a measurement of P_{XY} . In the expression above, superscripts in parentheses refer to the values of (A_N, A_K, A_D) . The variance, ΔP_{XY}^2 , is computed for the total signal, including Doppler. (Note that this does not affect the results significantly, as Doppler is a sub-dominant term.)

Assuming a Gaussian covariance matrix for the power spectrum signal—accurate enough on the large, linear scales we are interested in—the variance associated with a measurement of $P_{XY}(\mathbf{k})$ averaged in a given redshift bin reads

$$\Delta P_{XY}^2(\mathbf{k}) = \frac{1}{N_k} \left[\tilde{P}_{XY}(\mathbf{k}) \tilde{P}_{YX}(\mathbf{k}) + \tilde{P}_{XX}(\mathbf{k}) \tilde{P}_{YY}(\mathbf{k}) \right], \quad (11)$$

having defined $\tilde{P} = P + N$, with N the noise related to a measurement of P , and $N_k = 2\pi k^2 \Delta k \Delta \mu / k_f^3$. The latter quantity represents the number of independent modes available in the observed volume V , having introduced the fundamental frequency $k_f = 2\pi/V^{1/3}$. Lastly, Δk and $\Delta \mu$ denote the sizes of the (k, μ) -bins, whereas V depends on the redshift width, Δz .

In the case of the galaxy power spectrum, the noise power spectrum is a scale-independent, shot-noise term

due to galaxies discretely sampling the underlying continuous matter distribution. Specifically, we have $N_{XY}(\mathbf{k}; \bar{z}_i) \equiv N_{XY}(\bar{z}_i) = \delta_{(K)}^{XY} / \bar{n}_X(\bar{z}_i)$, with $\delta_{(K)}$ the Kronecker delta symbol and \bar{n}_X the mean (volumetric) galaxy number density in the i th redshift bin. Finally, it is worth noting that the variance of the faint-bright cross-correlation power spectrum, P_{FB} , is real, despite the signal itself being complex. This is due to the fact that $P_{XY} = P_{XY}^*$ for any pair of tracers.

In our analysis, we fix the largest wavenumber, k_{\max} , to $k_{\text{nl}} = 0.2 h \text{ Mpc}^{-1}$, viz. the scale at which non-linear effects take over the linear growth of structure at $z = 0$. This is a conservative approach, since k_{nl} is a redshift-dependent quantity, monotonically increasing with redshift; and, furthermore, there are available recipes to push at least to mildly non-linear scales. But our choice is motivated by the Doppler signal scaling with k^{-1} or k^{-2} , meaning that large wavenumbers will in practice not contribute to the detection of the relativistic signal. On the other hand, the smallest wavenumber, k_{\min} , is a critical quantity. We choose to fix it to the fundamental frequency, k_f . By definition, this quantity is survey-dependent, being determined by the redshift range and binning, and by the observed fraction of the sky, f_{sky} . For the sake of generality, we shall for now assume to be observing the entire sky, providing later on the reader with means to rescale our findings to any f_{sky} .

For the definition of the redshift ranges for *Model 1* and *Model 3*, we follow Maartens *et al.* [19], namely $z \in [0.7, 2.0]$ for the former and $z \in [0.9, 1.8]$ for the latter. However, since we are interested in the largest scales, we choose to increase the available volume by taking roughly twice thicker redshift bins, with $\Delta z \approx 0.2$ —but we shall also discuss different binning choices. This implies a total of 7 z -bins for *Model 1* and 5 z -bins for *Model 3*. Finally, we adopt 30 log-spaced k -bins in the range $k \in [k_{\min}, k_{\max}]$ and 10 μ -bins in the range $\mu \in [-1, 1]$. We have checked that the actual number of k - and μ -bins does not significantly affect the final results.

Illustratively, in Fig. 1 we display the detection significance for the relativistic Doppler term for the *Model 1* luminosity function. We consider two galaxy populations with $F_c = 2.0 \times 10^{-16} \text{ erg cm}^{-2} \text{ s}^{-1}$ and flux split between the two samples $F_s = 2.8 \times 10^{-16} \text{ erg cm}^{-2} \text{ s}^{-1}$. The value of F_s is chosen so that the faint and bright samples are almost equally populated. First of all, by comparing separately the orange (faint sample) and the green (bright sample) histograms to the blue (total sample) one, it is clear that a larger statistics—that is, the total sample, with the largest number density—does not imply a better measurement of the Doppler term. This happens because on the largest scales, where the Doppler contribution becomes non-negligible, shot-noise is not an issue. On the other hand, the larger \mathcal{E} and \mathcal{Q} (in absolute value), the larger the amplitude of the Doppler term α (see Eq. 2), and for both sub-samples the improvement of $\Delta\chi^2$ roughly compensates for the sparsity of the samples (except for the faint sample at low redshift). However, the average $\Delta\chi^2$ per redshift bin remains at most of order %, making any detection effectively unrealistic. Conversely, the use of the cross-correlation turns the situation around, thanks to the appearance of the $\propto k^{-1}$ term in Eq. (6). Indeed, per-bin $\Delta\chi^2$ values

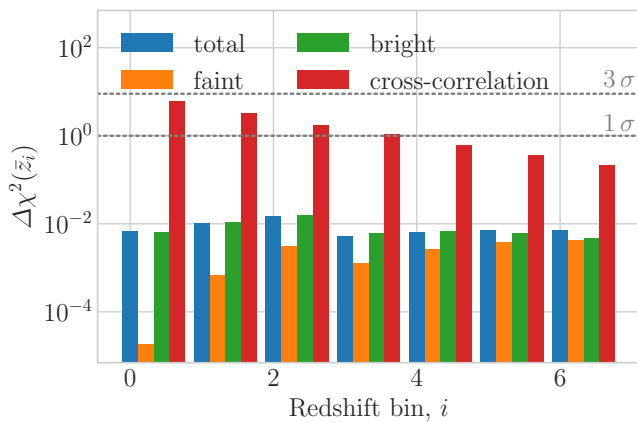


FIG. 1. Detection significance of relativistic Doppler contribution for a *Model 1* luminosity function. The $\Delta\chi^2$ variable is evaluated against a null hypothesis of no Doppler contribution in the galaxy power spectrum. Colour code: blue, orange, and green respectively for auto-correlation power spectrum of total, faint, and bright samples; red is for the faint-bright cross-correlation power spectrum.

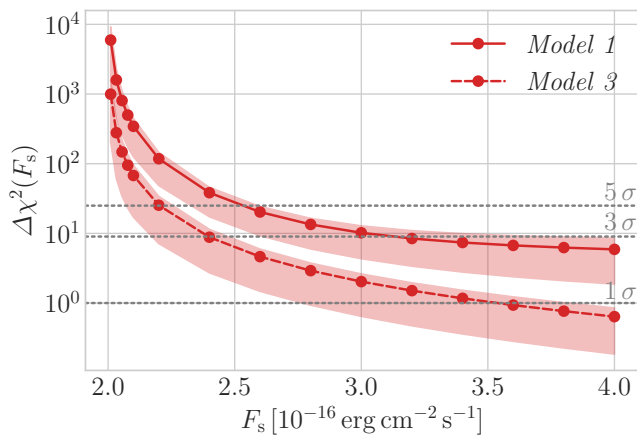


FIG. 2. Cumulative statistical significance of the detection of the relativistic Doppler effect associated with a faint-bright cross-correlation power spectrum measurement as a function of F_s . Solid curve is for *Model 1* and dashed curve for *Model 3*, whilst dotted lines mark 1σ , 3σ , and 5σ significance levels. Shaded areas around each curve bracket the dependence upon Δz , from ~ 0.05 (bottom edge) to ~ 0.3 (top edge).

are now well above unity at the lowest redshifts considered, with an average improvement of a factor 100–1000 over the auto-correlation power spectrum of the total sample.

Now, focussing on the most promising observable—the cross-correlation power spectrum—Fig. 2 shows the total $\Delta\chi^2$ associated with the detection of the relativistic Doppler effect, cumulative over all redshift bins, as a function of F_s . Results for both *Model 1* (solid curve) and *Model 3* (dashed curve) are reported now. The reference $\Delta z \approx 0.2$ is shown with lines and circle markers, whereas the shaded areas around each curve bracket the scenarios from narrow to wide redshift bins, namely $\Delta z \approx 0.05$ to 0.3 . As expected, the wider

bins the larger the detection significance, due to the increase in available volume. For the reference scenario, the cumulative $\sqrt{\Delta\chi^2}$ for *Model 1(3)* reaches readings above the 5σ detection threshold, if $F_s \leq 2.5(2.2) \times 10^{-16} \text{ erg cm}^{-2} \text{ s}^{-1}$. This definitively demonstrates the constraining power of the technique, when compared to *Model 1(3)* results for the three auto-correlations: $0.2(0.2)\sigma$ for the total sample; $0.1(0.2)\sigma$ for the faint sample; and $0.2(0.2)\sigma$ for the bright sample. These numbers refer to limiting fluxes as Fig. 1, i.e. flux cut $F_c = 2.0 \times 10^{-16} \text{ erg cm}^{-2} \text{ s}^{-1}$ and splitting flux $F_s = 2.8 \times 10^{-16} \text{ erg cm}^{-2} \text{ s}^{-1}$, so that the two faint/bright sub-samples have approximately the same number density.

Figure 2 also points out an improvement in the detection significance when F_s approaches F_c . That situation corresponds to an asymmetrical subdivision, with a faint sample much less populated than the bright one. This finding is in agreement with the recent Bonvin *et al.* [26], who looked at the dipole of the galaxy two-point correlation function as a proxy of the Doppler term. Such an increment looks reasonable due to the Q behaviour. Indeed, the modulating factor n_T/n_F in Eq. (7) actually boosts the magnification bias value for the faint population if $n_F \ll n_B$ and, in turn, the relativistic Doppler term in the cross-power spectrum.

Parameter constraints. We now move to estimate the error associated with a measurement of each of the contributions to the power spectrum, namely the three parameters we introduced before: the amplitude of the Newtonian term, A_N ; that of the Kaiser RSD contribution, A_K ; and that of the Doppler effect, A_D . Going back to Eq. (4), we include these dummy variables as amplitude parameters, whose fiducial values are fixed to $A_N = A_K = A_D = 1$. Then, the uncertainty on a measurement of them can be evaluated through an information matrix analysis. In the i th redshift bin, the information matrix for the parameter set $\theta = \{A_N, A_K, A_D\}$ reads

$$I_{\alpha\beta}(\bar{z}_i) = \sum_{m,n} \frac{1}{\Delta P_{XY}^2(k_m, \mu_n; \bar{z}_i)} \times \left[\frac{\partial P_{XY}(k_m, \mu_n; \bar{z}_i)}{\partial \theta_{(\alpha)}} \frac{\partial P_{XY}^*(k_m, \mu_n; \bar{z}_i)}{\partial \theta_{(\beta)}} \right]_{\theta=1}, \quad (12)$$

where parentheses around indexes denote symmetrisation, the variance is again given by Eq. (11), and the sum runs over all the configurations (k_m, μ_n) . Hence, the total Fisher matrix, cumulative over all redshift bins, is simply $I = \sum_i I(\bar{z}_i)$. Lastly, the cumulative marginal errors on $\{\theta_\alpha\}$ are given by $\sigma_{\theta_\alpha} = \sqrt{(I^{-1})_{\alpha\alpha}}$.

Analogously to Fig. 2, Fig. 3 shows the cumulative marginal error on the estimation of A_D , σ_{A_D} , as a function of F_s . As before, solid and dashed lines are for *Model 1* and *Model 3*, respectively, and shaded areas bracket $0.05 \leq \Delta z \leq 0.3$. Since the fiducial value is set to $A_D = 1$, we at least need $\sigma_{A_D} < 1$ in order to claim a detection of the relativistic contribution. For *Model 1* this condition is always verified, whereas for *Model 3* it is verified only if $F_s \leq 3.6 \times 10^{-16} \text{ erg cm}^{-2} \text{ s}^{-1}$. We clearly see the same asymmetrical behaviour of Fig. 2 w.r.t. the total galaxy population, i.e. the closer F_s to F_c , the higher the accuracy in the detection of the amplitude of the Doppler term. Furthermore, it is worth noting the relation be-

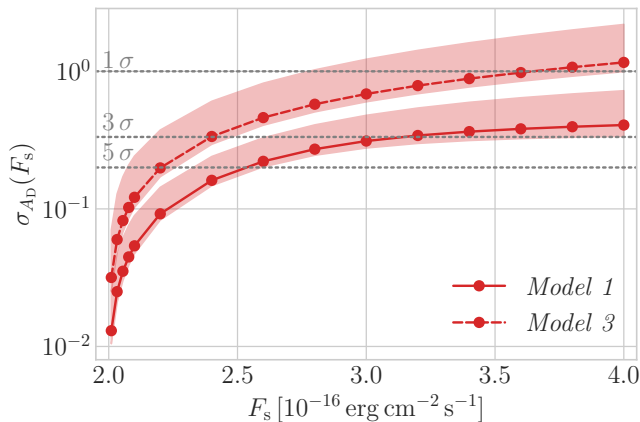


FIG. 3. Same as Fig. 2 for σ_{A_D} , i.e. the marginal error on a measurement of the Doppler amplitude, A_D . Note that limits of shaded areas are now reversed, with $\Delta z \simeq 0.05(0.3)$ being the top(bottom) edge.

tween the two statistical tools we adopt: because of the A_D definition, we have $\sqrt{\Delta\chi^2} \sim \sigma_{A_D}^{-1}$. This might come as unexpected, since we are considering two additional parameters on top of the Doppler amplitude, namely A_N and A_K , whose presence should in principle manifest itself in a loosening on the constraining power over A_D . However, since the real and imaginary components of a complex number are orthogonal to each other, A_D is effectively almost uncorrelated to either A_N or A_K , with correlation coefficients respectively amounting to, at most, 0.03(0.07) and 0.03(0.09) for *Model 1*(3).

Partial sky coverage. Let us remind the reader that the results hitherto presented refer to the idealistic case of full-sky observations. In truth, this is never the case, either because a ground-based telescope will have access only to a portion of the celestial sphere, or because even a space-born experiment will not be able to pierce through our own Galaxy, whose stars will block the line of sight and whose diffuse gas will absorb incoming radiation. Nonetheless, for the wide sky coverages usually envisioned for cosmological analyses, the effect of partial sky can be folded in by rescaling the volume V in Eq. (11) by the fraction of observed sky, f_{sky} .

For most applications, the effect of an $f_{\text{sky}} \neq 1$ on a measurement of P_{XY} can be thought of as a simple inflation of the error bars by a factor $f_{\text{sky}}^{-1/2}$. However, in the present case in which we seek to detect an effect relevant on the largest scales, we should also in principle account for the fact that a smaller volume directly translates into a larger fundamental frequency, k_f ; and that the fundamental frequency is the smallest wavenumber observable. Hence, any $f_{\text{sky}} \neq 1$ would call for a rerun of the analysis, with a larger k_{min} (which, we remind the reader, we fix equal to k_f) and, possibly, a different k -binning. However, we find that this effect is relevant only when looking at the differential, per-bin $\Delta\chi^2$ and σ_{A_D} , whilst it effectively cancels out in the cumulative ones. More quantitatively, the simple rescaling of the variance of Eq. (11) by f_{sky} works remarkably well, with discrepancies $< 5\%$ even for sky coverages as small as $f_{\text{sky}} \simeq 0.05$. Thanks to the validity of such scaling relation, our main results of Figs. 2 and 3 can

be easily related to any f_{sky} .

Discussion and conclusions. A measurement of a peculiar GR effect on cosmological scales would be an astonishing confirmation of the validity of Einstein’s theory in a regime where it is poorly probed experimentally. With the upcoming galaxy surveys, this wish looks set to become a reality, thanks to the unprecedented cosmic volumes probed, which will allow us to sample even the largest scales in structure of the Universe. In this work, we have presented forecasts for the detection of the relativistic Doppler term with galaxy power spectrum measurements, for both auto- and cross-correlations of various galaxy samples. Since the amplitude of such Doppler term differs according to the target galaxy population, we set to the task of optimising sample selection, for the search for a relativistic signature in cosmic structures.

In general, the comparison between auto- and cross-correlation measurements points out the supremacy of the latter, mostly due to the milder scale dependence of the Doppler term. The relativistic contribution seems to be relevant only on very large scales in the case of auto-correlation, nevertheless its presence in the imaginary part of the cross-power spectrum appears to be measurable even at somewhat intermediate scales [13]. Concerning the faint-bright cross-correlation, the differential Doppler detection significance, being around one order of magnitude larger over the entire redshift range than that found in the auto-correlation cases, shows that the most powerful constraints came from the lowest redshift bins [26].

Considering the whole redshift range, i.e. the cumulative detection significance, we are able to obtain a detection of the relativistic Doppler effect with a confidence level well above 5σ , by carefully selecting F_s , namely the value of the flux that splits the two sub-samples. Indeed, when the splitting flux decreases, the detection significance improves. For the cross-power spectrum between the faint and the bright populations, the 5σ detection is reached in the case of *Model 1*(3) at $F_s \simeq 2.5(2.5) \times 10^{-16} \text{ erg cm}^{-2} \text{ s}^{-1}$. Furthermore, results for the detection significance are confirmed by the estimation of the marginal error via the information matrix formalism. Regarding the lowest confidence level, the faint-bright cross-correlation appears to allow for a 1σ detection of the relativistic Doppler for both galaxy populations described by *Model 1* and *Model 3* luminosity functions for any F_s value we have tested and for $F_s \leq 3.6 \times 10^{-16} \text{ erg cm}^{-2} \text{ s}^{-1}$, respectively. The closer to the flux cut the splitting flux is, the smaller the marginal error becomes. In addition, a check on the impact of the statistical framework used—that is the width of the bins in z , μ , k —tells us that all the analyses presented are robust, in the sense that the results do not vary significantly if we vary the analysis set-up.

To conclude, the luminosity cut technique proposed by Bonvin *et al.* [10] appears to be very promising for power spectrum analyses, not only because it makes cross-correlation measurements possible using just one data set, but also because it can boost the relativistic contribution as long as the bright sample is more populated than the faint one. Note that the results presented here come, for the first time, from a fully self-consistent treatment of all the relevant observational quantities, such as the galaxy bias and the magnification and

evolution biases. We have been able to achieve this thanks to the implementation of analytical scaling relations calibrated on real data [see also 27].

Future studies will then have to assess the reliability of the strategy using simulated data. For instance, it will be important to assess how much some aspects be due to the modelling adopted. Also, we cannot clearly assume that Doppler detection improves monotonically as F_s approaches F_c , because at a certain point the faint sample could become too sparsely populated to extract information. Even in our analytical approach, we observe an order of magnitude worsening of the marginal errors associated with a measurement of the Newtonian and Kaiser terms (i.e. the of the parameters A_N and A_K) when we reach $F_s \simeq 2.01 \times 10^{-16} \text{ erg cm}^{-2} \text{ s}^{-1}$. This seems

meaningful, in the sense that it ensures us that we cannot excessively boost the Doppler contribution via depopulating the faint sample, because we would lose accuracy in estimating the dominant terms of the power spectrum. Furthermore, flux density measurements are subject to several technical details, like the angular size and the magnitude of the target galaxy, the exposure time, etc. For this reason, some issues might occur in the definition of the sub-samples, and thus caution might be needed in the choice of the splitting flux and in the estimation of the galaxy brightness uncertainty.

Acknowledgments. The authors would like to thank Chris Clarkson, Roy Maartens, and Camille Bonvin for their reading of the final draft of the manuscript, as well as to Nicolao Fornengo, for the useful questions raised during the presentation of earlier stages of FM's thesis, whence this work stemmed.

-
- [1] J. B. Holberg, *Journal for the History of Astronomy* **41**, 41 (2010).
- [2] I. I. Shapiro, G. H. Pettengill, M. E. Ash, M. L. Stone, W. B. Smith, R. P. Ingalls, and R. A. Brockelman, *Physical Review Letters*, **20**, 1265 (1968).
- [3] N. Ashby, *Physics Today* **55**, 41 (2002).
- [4] R. A. Hulse and J. H. Taylor, *The Astrophysical Journal Letters* **195**, L51 (1975).
- [5] J. M. Weisberg and J. H. Taylor, in *Binary Radio Pulsars*, Astronomical Society of the Pacific Conference Series, Vol. 328, edited by F. A. Rasio and I. H. Stairs (2005) p. 25, arXiv:astro-ph/0407149 [astro-ph].
- [6] Nanograv Collaboration, *The Astrophysical Journal Letters* **951**, L8 (2023), arXiv:2306.16213 [astro-ph.HE].
- [7] LIGO Scientific Collaboration and Virgo Collaboration, *Physical Review Letters* **116**, 061102 (2016), arXiv:1602.03837 [gr-qc].
- [8] T. Clifton, P. G. Ferreira, A. Padilla, and C. Skordis, *Physics Reports* **513**, 1 (2012), arXiv:1106.2476 [astro-ph.CO].
- [9] A. Joyce, L. Lombriser, and F. Schmidt, *Annual Review of Nuclear and Particle Science* **66**, 95 (2016), arXiv:1601.06133 [astro-ph.CO].
- [10] C. Bonvin, L. Hui, and E. Gaztañaga, *Phys. Rev. D* **89**, 083535 (2014), arXiv:1309.1321 [astro-ph.CO].
- [11] C. Bonvin, L. Hui, and E. Gaztanaga, *J. Cosmol. Astrop. Phys.* **2016**, 021 (2016), arXiv:1512.03566 [astro-ph.CO].
- [12] E. Gaztanaga, C. Bonvin, and L. Hui, *J. Cosmol. Astrop. Phys.* **2017**, 032 (2017), arXiv:1512.03918 [astro-ph.CO].
- [13] P. McDonald, *J. Cosmol. Astrop. Phys.* **2009**, 026 (2009), arXiv:0907.5220 [astro-ph.CO].
- [14] L. R. Abramo and D. Bertacca, *Phys. Rev. D* **96**, 123535 (2017), arXiv:1706.01834 [astro-ph.CO].
- [15] A. Challinor and A. Lewis, *Phys. Rev. D* **84**, 043516 (2011), arXiv:1105.5292 [astro-ph.CO].
- [16] E. Di Dio, R. Durrer, G. Marozzi, and F. Montanari, *J. Cosmol. Astrop. Phys.* **2016**, 016 (2016), arXiv:1510.04202 [astro-ph.CO].
- [17] E. Di Dio and F. Beutler, *J. Cosmol. Astrop. Phys.* **2020**, 058 (2020), arXiv:2004.07916 [astro-ph.CO].
- [18] C. Bonvin and R. Durrer, *Phys. Rev. D* **84**, 063505 (2011), arXiv:1105.5280 [astro-ph.CO].
- [19] R. Maartens, J. Fonseca, S. Camera, S. Jolicoeur, J.-A. Viljoen, and C. Clarkson, *J. Cosmol. Astrop. Phys.* **2021**, 009 (2021), arXiv:2107.13401 [astro-ph.CO].
- [20] R. Maartens, S. Jolicoeur, O. Umeh, E. M. De Weerd, C. Clarkson, and S. Camera, *J. Cosmol. Astrop. Phys.* **2020**, 065 (2020), arXiv:1911.02398 [astro-ph.CO].
- [21] P. Paul, C. Clarkson, and R. Maartens, *J. Cosmol. Astrop. Phys.* **2023**, 067 (2023), arXiv:2208.04819 [astro-ph.CO].
- [22] M. Martinelli, R. Dalal, F. Majidi, Y. Akrami, S. Camera, and E. Sellentin, *Mon. Not. Roy. Astron. Soc.* **510**, 1964 (2022), arXiv:2106.15604 [astro-ph.CO].
- [23] L. Pozzetti, C. M. Hirata, J. E. Geach, A. Cimatti, C. Baugh, O. Cucciati, A. Merson, P. Norberg, and D. Shi, *Astron. Astrophys.* **590**, A3 (2016), arXiv:1603.01453 [astro-ph.GA].
- [24] L. D. Ferramacho, M. G. Santos, M. J. Jarvis, and S. Camera, *Mon. Not. Roy. Astron. Soc.* **442**, 2511 (2014), arXiv:1402.2290 [astro-ph.CO].
- [25] H. Pan, D. Obreschkow, C. Howlett, C. d. P. Lagos, P. J. Elahi, C. Baugh, and V. Gonzalez-Perez, *Mon. Not. Roy. Astron. Soc.* **493**, 747 (2020), arXiv:1909.12069 [astro-ph.CO].
- [26] C. Bonvin, F. Lepori, S. Schulz, I. Tutusaus, J. Adamek, and P. Fosalba, arXiv e-prints, arXiv:2306.04213 (2023), arXiv:2306.04213 [astro-ph.CO].
- [27] J. Fonseca and S. Camera, *Mon. Not. Roy. Astron. Soc.* **495**, 1340 (2020), arXiv:2001.04473 [astro-ph.CO].